Light diffraction by $KTiOPO_4$, a quasi-one-dimensional ionic conductor, under a dc field

Hua-guang Yang, Shi-jie Gu, Zheng-yi Xu, Yong Zhu, and Yin-yuan Li
Institute of Physics, Academia Sinica, Beijing, China
(Received 26 May 1987)

Single crystals of $KTiOPO_4$ ($Pna2_1$) possess a quasi-one-dimensional (1D) ionic conductance with $\sigma_{\parallel}/\sigma_{\perp}\sim 10^4$, where $\sigma_{\parallel}$ and $\sigma_{\perp}$ are, respectively, the ionic conductivity parallel and normal to the c axis. A specimen was cut into a rectangular parallelepiped with edges parallel to the a, b, and c axes. Under a dc voltage applied to the c surfaces and a He-Ne laser beam incident normally to the a (or b) surface, a wide-angle diffraction band extending normal to the c axis was observed. If the electric displacement of the incident beam was parallel to the b (a) axis, that of the diffraction was parallel to the c axis, and vice versa. There was a delay time between the initial application of voltage and the appearance of the diffraction, and also between the removal of voltage and the disappearance of diffraction. This relaxation behavior suggests that the optical diffraction band and related phenomena are affected not directly by the ionic transportation but by the space charges left behind by the flow of charge carriers. Our theoretical analysis based on phase-type gratings composed of Fourier components of the distribution of space charges and on the electro-optic effect of the related internal field successfully explains all the interesting features of the diffraction band.

I. INTRODUCTION

In recent years, single crystals of $KTiOPO_4$ (abbreviated as KTP) have become increasingly important as a nonlinear optical material.[1] It is an electric polar crystal whose space group is $Pna2_1$ with $a=12.814$ Å, $b=6.404$ Å, and $c=10.616$ Å.[2] Its indices of refraction for $\lambda=6328$ Å are correspondingly $n_1=1.762\,14$, $n_2=1.771\,31$, and $n_3=1.864\,32$ as measured by Hu.[3] The optical axes are in the b plane and the angle between the optical axes is around 35°. The ionic conductivities measured by Bierlein and Arweiler[4] with a dc field parallel and normal to the c axis are, respectively,

$$\sigma_{\parallel}\sim 10^{-8}(\Omega\,\mathrm{cm})^{-1}\ ,$$

$$\sigma_{\perp}\sim 10^{-12}(\Omega\,\mathrm{cm})^{-1}\ .$$

It is the second quasi-one-dimensional (1D) ionic conductor available to us in single crystals.

α-$LiIO_3$ was the first quasi-1D ionic conductor ever subjected to serious research.[5] According to Zhu *et al.*[6] $\sigma_{\parallel}=3\times 10^{-9}(\Omega\,\mathrm{cm})^{-1}$ and $\sigma_{\perp}=1\times 10^{-14}(\Omega\,\mathrm{cm})^{-1}$ in this crystal. The anisotropy in conductance is about the same order of magnitude in α-$LiIO_3$ and KTP. Because of the almost unlimited supply of good single crystals of α-$LiIO_3$ to Chinese physicists, the characteristics of this crystal have been investigated by them in much detail.[5] Most of the published articles are not universally known. A number of novel phenomena were discovered in this material and they are undoubtedly related to quasi-1D characteristics in ionic conductance. Among them, the wide-angle light diffraction bands extending normal to the c axis,[7,8] the selective enhancement of neutron diffractions,[9] and the increase of the real part of the low-frequency dielectric constant ϵ_c' under a bias field[6] are most interesting and have been investigated in detail. From the time delay between the appearance of these phenomena and the initial application of a voltage as well as that between their disappearance and the removal of the voltage, the effect may be attributed to space charges left behind by the 1D ionic flow. All the interesting characteristics of the light diffraction bands have been successfully interpreted by a theory based on phase-type gratings composed of the Fourier components of the distribution of space charges, and the eletro-optic effect of the induced internal field.[10] From further studies using polarizing microscopy[11] and careful analysis,[12] we are fully convinced that the novel phenomena mentioned above can be found only in quasi-1D ionic conductors.

In this paper we report on the observation of optical diffraction bands in a KTP single crystal under a dc voltage. They extend to wide angles and are normal to the c axis as expected. The envelope of the diffracted intensity is also consistent with the theoretical treatment. We conclude that the phenomena, which we have attributed to the accumulation of space charges, are not unique to α-$LiIO_3$ but must be considered a common characteristic of 1D ionic conductors. Our studies have produced an additional chapter[5,12] on the physics of one dimension.[13]

II. EXPERIMENT

The specimen, a good KTP single crystal grown from flux melt, was cut into a rectangular parallelepiped with the three pairs of surfaces parallel to the crystallographic planes a, b, and c, respectively. The orientations of the edges are accurate within 1°. After polishing, the crystals linear dimensions are $2.6\times 3.7\times 3.1$ mm^3 along the a, b, and c axes. The direction of P_s, the spontaneous polarization, is determined by the static piezoelectric effect. According to the international convention, the outwardly drawn normal to the c surface which becomes positively charged under a tensile stress, is the $+c$ direction.

An optical beam from a He-Ne laser with stabilized power of 0.5 mW was polarized and normally incident to the a surface of the specimen. A dc voltage was applied to the c surfaces which were covered with silver paste for good electrical contact. The transmitted spot and diffraction band were exhibited on a screen, and photographed or recorded by a photomultiplier. After a lag time from the initial application of the dc voltage in the c direction, a wide-angle diffraction band extending normal to the c axis appears. The angular distribution of intensity changes smoothly but shows disordered fine structure. The polarization of the diffracted light is different from that of the incident light. Precisely speaking, we found that the electric vector of the diffracted light is parallel to the c axis when that of the incident light is parallel to the b axis, and that the former is parallel to the b axis when the latter is parallel to the c axis. Figure 1 is a photograph taken at 30 cm from the specimen, under the action of 100-V dc voltage, i.e., $\bar{E}=323$ V/cm, with the incident beam polarized with its electric vector parallel to the c axis. As shown in Fig. 1, the envelope of the intensity distribution with respect to the transmitted beam is symmetric, i.e., $I(-\theta)=I(\theta)$, where θ is the scattering angle. It has a minimum of intensity at $\theta=0$, i.e., at the transmitted spot. Two intensity maxima are found symmetrically at $\theta_{\text{out}}=\pm 4.8°$. When the incident beam is normal to the b instead of a surface, the diffraction band is found extending also normal to the c axis, with a similar change of polarization states and a similar intensity distribution to that found with the incident beam normal to the a surface.

We list below the dependence of the experimental findings on various conditions, such as the temperature of the specimen, the strength and frequency of applied voltages, the direction of $\bar{E}$, etc.

(1) The total intensity of the diffracted light or the intensity at a certain scattering angle $I(\theta)$ increases with the applied voltage, i.e., with the average field strength $\bar{E}$.

(2) The time delay between the initial application of voltage and the appearance of diffraction and that between the removal of the voltage and the disappearance of the diffraction increases with decreasing temperature. At $T<195$ K the time delay becomes practically infinite for an observer. We call this effect "freezing." As a consequence, when the temperature of the specimen decreases below 195 K the diffraction band remains steady after the removal of the voltage. On the other hand, when we apply the dc voltage after the specimen is chilled down to 195 K or lower, the diffraction does not appear at all, but it gradually gains intensity as the specimen is warmed up.

(3) Using a low-frequency ac field, the intensity of the diffracted beam becomes weaker with the increase of frequency. In our experiment the diffraction band can barely be seen by eye when the frequency is 0.5 Hz and the ac peak voltage is 150 V.

(4) No diffraction can be detected at all if the voltage is applied to the a or b surfaces.

(5) Instead of looking at the diffraction bands, we observed, using a polarizing microscope and crossed polarizers, a bundle of bright straight lines parallel to the c axis and randomly distributed beneath the a surface (Fig. 2). This feature is not limited to one focal plane of the microscope but appears over the whole volume.

Similar characteristics were also found in α-$LiIO_3$. The straight lines were identified with the grating lines of the system of phase-type gratings. The onset of accumulation starts at the electrodes[11,14] where the interstitial Li^+ ions and Li^+ vacancies collect at the cathode and the anode, respectively, under the driving force, but a number of them are not able to discharge at the electrodes. The accumulation of charge must be linear along the c axis, since there is very little opportunity for the ions to move sideways. Liu *et al.*[14] also revealed that the straight lines are actually charged. For KTP we should reach the same conclusion. Zhang *et al.*[15] showed earlier that in α-$LiIO_3$ both the positive and negative charge carriers, i.e., interstitial Li^+ and Li^+ vacancies, are nearly equally active. We have not yet determined whether one or two kinds of charge carriers are active in KTP.

On the other hand, there are differences in the time dependence of the diffraction and current in KTP and α-$LiIO_3$ after the application of a dc voltage at room temperature. The rate of elongation of the straight fibers is much faster in KTP than that observed in α-$LiIO_3$. When the diffraction intensity was measured at

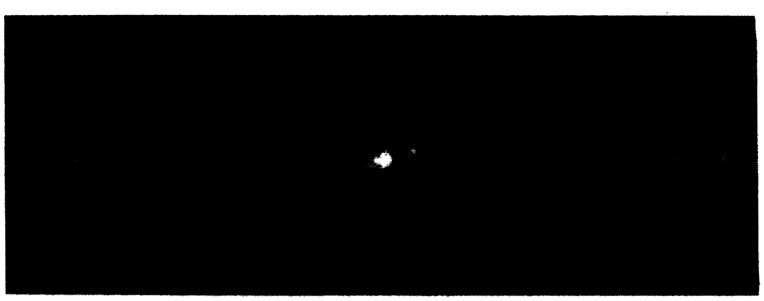

FIG. 1. Diffraction band at 30 cm of the KTP specimen under 100-V dc voltage applied on the c surfaces. The incident beam from a He-Ne laser is normal to the a surface. The incident beam's electric vector is parallel to the c axis and that of the diffracted light parallel to the b axis.

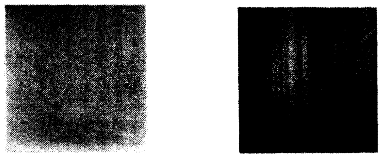

FIG. 2. Image of the linear space-charge accumulation underneath the a surface taken by a polarizing microscope with a crossed analyzer ($\times 100$). On the left, $V=0$; on the right, $V=100$ V.

room temperature and with $\bar{E}=97$ V/cm by a photomultiplier, it rose to a peak in about 20 sec. It fluctuated slightly and then it generally decreased to zero with the dc voltage still applied. The current flowing through the specimen showed a similar variation. However, a fairly strong diffraction intensity reappeared after vanishing to zero, if we reversed the applied dc field. In α-$LiIO_3$ the diffraction reached its full intensity in a half hour or so after the voltage was applied and it remained almost steady for hours as long as the voltage was not removed. Even after the removal of the voltage, the brightness of the diffraction band diminished slowly over a period of several hours. These differences might be tentatively understood as follows. Since $\sigma_\parallel$ and $\sigma_\perp$ of KTP are larger than those of α-$LiIO_3$ by 1 and 2 orders of magnitude, respectively, many more charge carriers in KTP are driven at a time to the cathode or both the electrodes than those in α-$LiIO_3$ under an equal $\bar{E}$. After a shorter time delay an appreciable number of carriers are blocked from discharging at the electrodes and the rate of elongation of the linear accumulation of space charges must be faster in KTP. As the density of space charges reaches a higher degree of inequilibrium, the current decreases even with the applied voltage remaining unchanged. At this stage the charges may move sideways away from the grating lines under the action of E_x and E_y induced from the volume distribution of space charges (cf. Sec. III). So the diffraction band fades gradually without the removal of voltage. When we reverse the applied dc field, a fairly strong diffraction intensity reappears, after it had vanishes. Naturally, this should happen, since the carriers earlier blocked at the electrodes now flow in the reversed direction and once again the linear accumulation of space charges must come into being. From our earlier experimentation with α-$LiIO_3$, we notice that the relaxation behavior of KTP at room temperature is rather similar to that of α-$LiIO_3$ at higher temperatures, e.g., 100 °C.

III. THEORY

Gu and Li[10] have worked out a theory to treat the light diffraction bands observed in α-$LiIO_3$ for the $o \to e$ and $e \to o$ diffraction bands. Here o and e denote, respectively, the ordinary and extraordinary light, and $o \to e$ means that the incident beam is the o light and the diffracted e light. This theory successfully explains all the characteristics of the phenomena and yields numerical results in quantitative agreement with experimental data. In the present article we will apply this theory to the interpretation of our experimental findings with a KTP specimen. Since this crystal is optically biaxial, the terms o and e are no longer meaningful. For each beam there are two polarization states with their electric displacement vectors normal to the wave vector. $\mathbf{K}_i/|\mathbf{K}_i|$, $\hat{\mathbf{e}}_i^{(1)}$, and $\hat{\mathbf{e}}_i^{(2)}$ form a right-handed system of axes.

It is necessary to give here a brief outline of the formulation. The grating effect is an outcome of the Fourier components of the space-charge distribution. In general we have

$$\delta\rho(\mathbf{r}) = \delta\rho \int H(\mathbf{K}) \sin(\mathbf{K}\cdot\mathbf{r}) d\mathbf{K} . \tag{1}$$

The random fluctuation $\delta\rho(\mathbf{r})$ is treated as the integration of sinusoidal distribution $\sin(\mathbf{K}\cdot\mathbf{r})$ weighted by $H(\mathbf{K})$ over all possible wave vectors. Since the diffraction bands extend in the xy plane, we have $K_z=0$. ($|\mathbf{K}| \neq 0$ is required for keeping neutrality of the total charge in the crystal.) In this way, the variations of the electric field and dielectric tensor may also be regarded as the integration of the corresponding sinusoidal distribution. Therefore, this corresponds to the existence of volume phase gratings with all possible wave vectors $\mathbf{K}$ in the xy plane for the incident light. An incident light beam with the wave vector $\mathbf{K}_1$ is diffracted by the $\mathbf{K}$ grating into the beam $\mathbf{K}_2$ in accordance with the Bragg condition

$$\mathbf{K}_1 + \mathbf{K} = \mathbf{K}_2 , \tag{2}$$

where

$$|\mathbf{K}_1| = 2\pi n_1^{(l)}/\lambda, \quad |\mathbf{K}_2| = 2\pi n_2^{(l)}/\lambda, \quad |\mathbf{K}| = 2\pi/\Lambda_{\mathbf{K}} . \tag{3}$$

λ is the wavelength in vacuum and Λ_k is the spacing parameter related to $\mathbf{K}$. The refractive indices $n_1^{(l)}$ and $n_2^{(l)}$ are related to the polarization of the beams, where $l=1$ and 2 indicate the two polarization states.

However, the $H(\mathbf{K})$ is yet completely unknown. Physically it is reasonable to consider $H(\mathbf{K})$ changing rapidly with $\mathbf{K}$ in a random fashion but with the envelope a smooth curve. From Poisson's equation, the field induced by the $\mathbf{K}$ component of space-charge density

$$\delta\rho_{\mathbf{K}}(\mathbf{r}) = \delta\rho \sin(\mathbf{K}\cdot\mathbf{r}) \tag{4}$$

is

$$\delta E_i^{\mathbf{K}}(\mathbf{r}) = -(\epsilon_{ij}^{-1} k_j / |\mathbf{K}|) \delta\rho \cos(\mathbf{K}\cdot\mathbf{r})$$
$$= \delta E_i^{\mathbf{K}} \cos(\mathbf{K}\cdot\mathbf{r}) , \tag{5}$$

where k_j is the jth component of $\mathbf{K}$ divided by $|\mathbf{K}|$.

The linear electro-optic effect induces a change in ϵ_{ij}

$$\delta\epsilon_{ij}^{\mathbf{K}}(\mathbf{r}) = \delta\epsilon_{ij}^{\mathbf{K}} \cos(\mathbf{K}\cdot\mathbf{r}) , \tag{6}$$

with

$$\delta\epsilon_{ij}^{\mathbf{K}} = -\epsilon_{ih}\gamma_{hkl}\epsilon_{kj}\delta E_l^{\mathbf{K}} , \tag{7}$$

since by definition

$$(\delta\epsilon^{-1})_{ij}=\gamma_{ijl}\delta E_l \ . \tag{8}$$

The Einstein summation convention has been and will be used throughout this paper. Now let us apply the general approach, previously adopted by Gu and Li[10] for α-$LiIO_3$, to KTP. For $mm2$ symmetry, only the tensor components γ_{13}, γ_{23}, γ_{33}, γ_{42}, and γ_{51} are nonzero. We also have $K_z=0$ and $\delta E_z=0$. Although the adoption of $K_z=0$ here is purely phenomenological, from the linear accumulation of space charges observed by a polarizing microscope, we have $\delta\rho(\mathbf{r})=\delta\rho(x,y)$, and $K_z=0$ follows. Naturally the diffraction band should appear normal to the z axis.

Consequently we have

$$\begin{aligned}
(\delta\epsilon^{-1})_{11}&=\gamma_{13}\delta E_z=0 \ ,\\
(\delta\epsilon^{-1})_{22}&=\gamma_{23}\delta E_z=0 \ ,\\
(\delta\epsilon^{-1})_{33}&=\gamma_{33}\delta E_z=0 \ ,\\
(\delta\epsilon^{-1})_{12}&=(\delta\epsilon^{-1})_{21}=0 \ ,\\
(\delta\epsilon^{-1})_{13}&=(\delta\epsilon^{-1})_{31}=\gamma_{51}\delta E_x \ ,
\end{aligned} \tag{9}$$

and

$$(\delta\epsilon^{-1})_{23}=(\delta\epsilon^{-1})_{32}=\gamma_{42}\delta E_y \ .$$

According to Petrov *et al.*[16] the efficiency of light diffraction by a phase-type grating is given by

$$\eta=\sin^2\left[\left[\frac{\pi}{\lambda}\right]^2\frac{|e_{1i}\delta\epsilon_{ij}e_{2j}|}{(K_{1x}K_{2x})^{1/2}}d\right] , \tag{10}$$

where d is the thickness of the grating, and K_{1x} and K_{2x} are the projections of incident and diffracted (inside the crystal) wave vectors in the direction normal to the incident surface. Here we have not taken into account any contributions from multiple diffraction. The subscripts 1 and 2 stand, respectively, for the incident and diffracted beams inside the medium, and $\hat{\mathbf{e}}_1$ and $\hat{\mathbf{e}}_2$ are the unit vectors in the directions of the electric displacements. In our case both $\mathbf{K}_1$ and $\mathbf{K}_2$ are in the plane normal to the c axis.

For each $\mathbf{K}$ grating it is good enough to approximate $\sin x$ by x in (10). Therefore, we evaluate

$$C^{(ll')}=|e_{1i}^{(l)}\delta\epsilon_{ij}e_{2j}^{(l')}|/(K_{1x}K_{2x})^{1/2} \tag{11}$$

instead of (10). Since $E_z=0$, $\mathbf{K}$ must be in the xy plane. Let $\mathbf{K}_1$ make angle ϕ with the x axis and let θ be the angle between $\mathbf{K}_1$ and $\mathbf{K}_2$ (cf. Fig. 3). $\mathbf{K}_1$, $\mathbf{K}_2$, and $\mathbf{K}$ make up the sides of a triangle (Bragg equation). We shall use the right-hand coordinate system. The sign of ϕ is defined as + or − depending on whether $\hat{\mathbf{i}}\times\mathbf{K}_1$ is in + or − direction relative to the z axis. Similarly, the sign

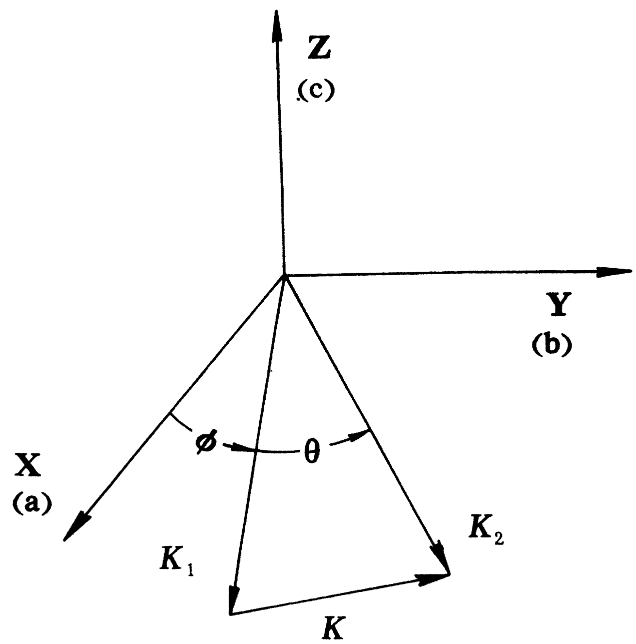

FIG. 3. Wave vectors of the incident and diffracted light in the xy plane and the Bragg triangle.

of θ is related to $\mathbf{K}_1\times\mathbf{K}_2$ by the same rule.

Now we evaluate $C^{(ll')}(\phi,\theta)$ as follows. In the expressions obtained below the factor $\delta\rho\epsilon_{33}\gamma_{51}(\lambda^2/4\pi^2)$ is neglected. We write

$$\mathbf{K}_1=[\hat{\mathbf{i}}\cos\phi+\hat{\mathbf{j}}\sin\phi]\,|\mathbf{K}_1| \ , \tag{12}$$

$$\mathbf{K}_2=[\hat{\mathbf{i}}\cos(\phi+\theta)+\hat{\mathbf{j}}\sin(\phi+\theta)]\,|\mathbf{K}_2| \ , \tag{13}$$

$$\hat{\mathbf{e}}_1^{(1)}=-\hat{\mathbf{i}}\sin\phi+\hat{\mathbf{j}}\cos\phi \ , \tag{14}$$

$$\hat{\mathbf{e}}_2^{(1)}=-\hat{\mathbf{i}}\sin(\phi+\theta)+\hat{\mathbf{j}}\cos(\phi+\theta) \ , \tag{15}$$

$$\hat{\mathbf{e}}_1^{(2)}=\hat{\mathbf{e}}_2^{(2)}=\hat{\mathbf{k}} \ , \tag{16}$$

with

$$n_1^{(2)}=n_2^{(2)}=n_3 \ ,$$

$$n_1^{(1)}=\left[\left[\frac{\cos\phi}{n_2}\right]^2+\left[\frac{\sin\phi}{n_1}\right]^2\right]^{-1/2} , \tag{17}$$

$$n_2^{(1)}=\left[\left[\frac{\cos(\phi+\theta)}{n_2}\right]^2+\left[\frac{\sin(\phi+\theta)}{n_1}\right]^2\right]^{-1/2} , \tag{18}$$

and the latter two will simply be denoted as $n(\phi)$ and $n(\theta+\phi)$, respectively. From Fig. 3 we easily see that

$$k_1=[\,|\mathbf{K}_2|\sin(\theta+\phi)-|\mathbf{K}_1|\sin\phi]/|\mathbf{K}| \ , \tag{19}$$

$$k_2=-[\,|\mathbf{K}_2|\cos(\theta+\phi)-|\mathbf{K}_1|\cos\phi]/|\mathbf{K}| \ . \tag{20}$$

Substituting (12)–(20) into (11) one easily gets

$$C^{(12)}(\phi,\theta)=\{a\cos\phi[n_3\sin(\theta+\phi)-n(\phi)\sin\phi]-\sin\phi[n_3\cos(\theta+\phi)-n(\phi)\cos\phi]\}$$
$$\times\{A^{(12)}(\phi,\theta)[n_3n(\phi)\cos\phi\cos(\theta+\phi)]^{1/2}\}^{-1} \ , \tag{21}$$

$$C^{(21)}(\phi,\theta)=\{a[\cos(\theta,\phi][n(\theta+\phi)\sin(\theta+\phi)-n_3\sin\phi]-[\sin(\theta+\phi)][n(\theta+\phi)\cos(\theta+\phi)-n_3\cos\phi]\}$$
$$\times\{A^{(21)}(\phi,\theta)[n_3 n(\theta+\phi)\cos\phi\cos(\theta+\phi)]^{1/2}\}^{-1}, \quad (22)$$

and

$$C^{(11)}(\phi,\theta)=C^{(22)}(\phi,\theta)=0, \quad (23)$$

where

$$A^{(12)}(\phi,\theta)=n_3^2+[n(\phi)]^2-2n_3n(\phi)\cos\theta, \quad (24)$$

$$A^{(21)}(\phi,\theta)=n_3^2+[n(\theta+\phi)]^2-2n_3n(\theta+\phi)\cos\theta, \quad (25)$$

and

$$a=\gamma_{42}/\gamma_{51}. \quad (26)$$

We shall reduce expressions (21) and (22) to correspond to the geometrical arrangements adopted in our experiment (Sec. II).

(1) For $\mathbf{K}_1$ normally incident to the a surface, $\phi=0$, we have

$$C_x^{(12)}(\theta)=(an_3\sin\theta)/(n_2^2+n_3^2-2n_2n_3\cos\theta)(n_2n_3\cos\theta)^{1/2}, \quad (27)$$

$$C_x^{(21)}(\theta)=\sin\theta[(a-1)n(\theta)\cos\theta+n_3](\{[n(\theta)]^2+n_3^2-2n(\theta)n_3\cos\theta\}[n(\theta)n_3\cos\theta]^{1/2})^{-1}. \quad (28)$$

(2) For $\mathbf{K}_1$ normally incident to b surface, $\phi=\pi/2$, then the denominator of Eq. (11) must be replaced as $[K_{1y}K_{2y}]^{1/2}$. Let $\phi=(\pi/2)+\phi'$. Equations (21) and (22) may be written in terms of ϕ' and θ. By putting $\phi'=0$, we obtain

$$C_y^{(12)}(\theta)=(n_3\sin\theta)/(n_1^2+n_3^2-2n_1n_3\cos\theta)[n_1n_3\cos\theta]^{1/2}, \quad (29)$$

$$C_y^{(21)}(\theta)=\sin\theta[(1-a)n'(\theta)\cos\theta+an_3](\{n_3+[n'(\theta)]^2-2n_3n'(\theta)\cos\theta\}[n_3n'(\theta)\cos\theta]^{1/2})^{-1}, \quad (30)$$

where

$$n'(\theta)=n(\theta+\pi/2)=\left[\left(\frac{\cos\theta}{n_1}\right)^2+\left(\frac{\sin\theta}{n_2}\right)^2\right]^{-1/2}. \quad (31)$$

Evidently for $\phi\neq0$ or $\pi/2$, the diffractions $|C^{(12)}(\phi,\theta)|^2$ and $|C^{(21)}(\phi,\theta)|^2$ are not symmetric in θ, but for any ϕ and θ the change of polarization states during diffraction is such that $\hat{e}^{(1)}\rightarrow\hat{e}^{(2)}$ or vice versa, as long as the incident beam is normal to the c axis.

It is interesting to compare the experimental findings with the above theoretical results.

(1) Since $C^{(11)}(\phi,\theta)=C^{(22)}(\phi,\theta)=0$, only the two $\hat{e}^{(1)}\rightarrow\hat{e}^{(2)}$ and $\hat{e}^{(2)}\rightarrow\hat{e}^{(1)}$ bands appear. They were investigated separately in the present experiment by using polarizers, although due to the small size of the specimen used, the observations were limited to the cases of $\phi=0$ and $\pi/2$. Evidently, $e_i^{(1)}$ and $e_i^{(2)}$ are analogous to the o light and e light in a uniaxial crystal such as α-$LiIO_3$.

(2) For both $\hat{e}^{(1)}\rightarrow\hat{e}^{(2)}$ and $\hat{e}^{(2)}\rightarrow\hat{e}^{(1)}$ bands the intensity distribution is symmetric with respect to $\theta=0$, i.e., $I(\theta)=I(-\theta)$ as can be seen from (27)–(30), since $I(\theta)\propto|C(\theta)|^2$.

(3) From (27)–(30) the diffraction intensity should vanish at $\theta=0$, i.e., at the transmitted spot. This is clearly shown in Fig. 1. We notice that the diffracted angle of zero intensity is not affected by the weight factor $H(\mathbf{K})$ of Eq. (1).

(4) In Fig. 1 the diffraction band shows a quasicontinuity in intensity changing with θ. The details of this disordered, spotty fine structure (cf. Fig. 1) can be easily registered by using a photomultiplier. Our record displays a rapid fluctuation in intensity with scattering angle. The same kind of fluctuation in intensity was also observed in the diffraction band of α-$LiIO_3$ and published in Ref. 7. The existence of fine structure confirms our physical intuition on the character of $H(\mathbf{K})$ as the weight factor in Eq. (1).

(5) In Fig. 1 the intensity shows two maxima at $\theta_{out}=\pm4.8°$ which is $\theta=\pm2.7°$ inside the crystal. Since both $C^{(12)}(\theta)$ and $C^{(21)}(\theta)$ have no maxima near $\theta=\pm2.7°$, we should look into the weight factor $H(\mathbf{K})$ for an explanation. $|\mathbf{K}|=0.12(2\pi/\lambda)$ for $\theta=2.7°$. With $\lambda=0.6328$ μm the spacing of the grating is about $\Lambda=5$ μm. Roughly speaking, the lines of space-charge accumulation shown in Fig. 2 possess a high probability of finding two of them 5 μm apart.

(6) From (28) there should be zero diffraction intensity in the $\hat{e}^{(2)}\rightarrow\hat{e}^{(1)}$ band for $\phi=0$ in addition to the zero when $\theta=0$, if the following condition is satisfied:

$$\cos\theta=n_3/(1-a)n(\theta).$$

However, this is impossible, since according to Ref. 4, $a=\gamma_{42}/\gamma_{51}=1.3$. Similarly, for the $\hat{e}^{(2)}\rightarrow\hat{e}^{(1)}$ band with incident beam along b axis ($\phi=\pi/2$ or $\phi'=0$)

$$\cos\theta=an_3/(a-1)n'(\theta)$$

also has no solution. Experimentally we observed no zero intensity other than the one at $\theta=0$ for both cases.

The general treatment in which the formulas for $C^{(ll')}(\alpha,\phi,\theta)$ are obtained will not be given in this paper because of the extremely lengthy and complicated calculation. Here, α is the angle between the incident beam and the c axis, and ϕ is the angle between the projection of the incident beam on the xy plane and the a axis. Qualitatively we have learned that as α deviates from $\pi/2$, i.e., the incident beam is no longer perpendicular to the c direction, $C^{(11)}$ and $C^{(22)}$ become nonvanishing. Let $\hat{\mathbf{e}}^{(1)}$ be the polarization state whose projection in the c direction is shorter than the projection of $\hat{\mathbf{e}}^{(2)}$. As α deviates appreciably from $\pi/2$, $C^{(22)}$ may become as strong as $C^{(12)}$ and $C^{(21)}$, but $C^{(11)}$ should be weaker by 2 orders of magnitude. These qualitative remarks are analogous to the explicit expressions given for the $o \Longleftrightarrow e$, $e \rightarrow e$, and $o \rightarrow o$ bands of α-$LiIO_3$.[10,17] The $o \rightarrow o$ band always vanishes as long as multiple scattering is neglected. With specimens of cm^3 size the experimentation on α-$LiIO_3$ was carried out on all conceivable cases, including $\alpha \neq \pi/2$ as well as a z-cut specimen with the two transmitting surfaces not parallel and not containing the c axis, etc. There, all the experimental findings were in good agreement with theoretical analyses qualitatively and also quantitatively whenever numerical data were available. However, more general geometrical arrangements in experimentation on KTP can be carried out only when good specimens of large size become available.

IV. CONCLUDING REMARKS

As related in Sec. I, long-term research on α-$LiIO_3$ under a dc field has been extremely fruitful in exposing special nature of space-charge effects in 1D ionic conductors. However, it was the only example of its kind. Among the novel phenomena discovered, the light diffraction bands were experimentally investigated and theoretically analyzed in great detail. After this paper was written, Yang[18] performed a neutron diffraction experiment on the same KTP specimen under a dc field parallel to the c axis. He found the same anisotropic selective enhancement observed in α-$LiIO_3$.[9]

We should mention that the physical factors behind our optical-diffraction phenomena are analogous to the photorefractive effect.[19] When one of the photorefractive crystals, such as $LiNbO_3$, $BaTiO_3$, $Bi_{12}SiO_{20}$, etc., is illuminated by a light beam with suitable wavelengths, photoelectrons are generated which migrate in the lattice and are subsequently trapped at new sites. The resulting space charges give rise to an electric-field strength distribution in the material which changes the dielectric tensor via the electro-optic effect. The fluctuation of electrons and/or holes is responsible for the photorefractive effect, while the interstitial ions and/or ion vacancies are responsible for the effect described in this paper.

Finally, we should like to remark that space charges are commonly involved in ionic conductance, yet for the materials with isotropic ionic conductivity, their distribution is homogeneous. There exist quasi-2D ionic conductors of which the ratio $\sigma_{\perp}/\sigma_{\parallel}$ approaches the same order of magnitude as that of $\sigma_{\parallel}/\sigma_{\perp}$ in 1D ionic conductors. Perhaps our future project of investigating materials of this kind with a bias field in the plane of higher conductivity might also be fruitful.

ACKNOWLEDGMENT

We are grateful to the financial support in part by the National Science Foundation of China under Grant No. 1860871.

[1]F. C. Zumstag, J. D. Bierlein, and T. E. Gier, J. Appl. Phys. **47**, 4980 (1976).

[2]L. Tordjman, R. Masse, and J. C. Guitel, Z. Kristallogr. Mineral. **139**, 103 (1974).

[3]B. Q. Hu (private communication).

[4]J. D. Bierlein and C. B. Arweilar, Appl. Phys. Lett. **49**, 917 (1986).

[5]Y. Y. Li, in *Advances in Science of China*, Vol. 1 of *Physics*, edited by H. Y. Zhu, G. Z. Zhou, and L. Z. Fang (Science Press, Beijing, 1985), p. 45.

[6]Y. Zhu, D. F. Zhang, and X. M. Cheng, Atca Phys. Sin. **26**, 115 (1977).

[7]H. G. Yang, Acta Phys. Sinica **29**, 1039 (1980).

[8]Z. Y. Xu, H. G. Yang, and Y. Y. Li, Sci. Sin. (English ed.), **26**, 637 (1983).

[9]Z. Yang, S. W. Neu, and Y. F. Cheng, Sci. Sin. (English ed.), **22**, 1000 (1979).

[10]S. J. Gu and Y. Y. Li, Acta Phys. Sin. **32**, 888 (1983) [Chin. Phys. **4**, 260 (1984)].

[11]G. Y. Zhang, J. Liu, and S. T. Feng, Acta Phys. Sin. **33**, 710 (1984).

[12]Y. Y. Li, Chin. Phys. Lett. **1**, 49 (1984).

[13]For example, *Physics in One Dimension,* edited by J. Bernaseoni, and T. Schneider (Springer-Verlag, Berlin, 1981).

[14]J. Liu, J. S. Xie, S. T. Feng, G. Y. Zhang, and Z. K. Wu, Acta Phys. Sin. **36**, 1199 (1987).

[15]A. D. Zhang, S. F. Zhao, A. Y. Xie, and Z. Y. Xu, Acta Phys. Sin. **29**, 1158 (1980) [Chin. Phys. **1**, 923 (1981)].

[16]M. H. Petrov, T. G. Pencheva, and S. I. Stepanov, J. Opt. (Paris), **12**, 287 (1981).

[17]S. J. Gu and Y. Y. Li, Acta Phys. Sin. **32**, 900 (1983) [Chin. Phys. **4**, 273 (1984)].

[18]Z. Yang, Chin. Phys. Lett. (to be published).

[19]P. Günter and H. J. Eichler, in *Electro-optic and Photorefractive Materials,* edited by P. Günter (Springer, Berlin, 1987), p. 206.

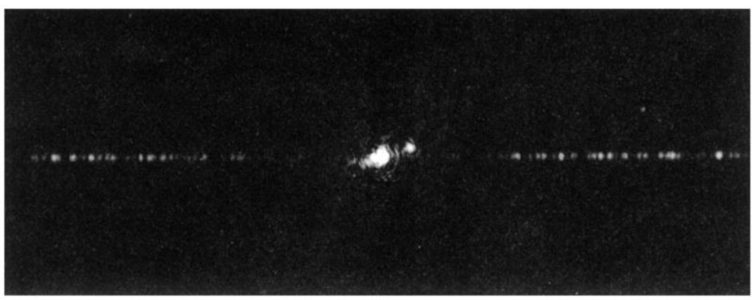

FIG. 1. Diffraction band at 30 cm of the KTP specimen under 100-V dc voltage applied on the *c* surfaces. The incident beam from a He-Ne laser is normal to the *a* surface. The incident beam's electric vector is parallel to the *c* axis and that of the diffracted light parallel to the *b* axis.

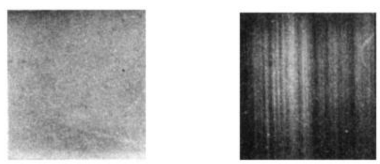

FIG. 2. Image of the linear space-charge accumulation underneath the *a* surface taken by a polarizing microscope with a crossed analyzer ($\times 100$). On the left, $V=0$; on the right, $V=100$ V.